

FRACTAL ANALYSIS ON MORPHOLOGY OF LASER IRRADIATED VANADIUM SURFACES UNDER DIFFERENT AMBIENT

Zs. Szkiva¹, Á. M. Bálint², M. Füle³, L. Nánai²

¹*Department of Experimental Physics, University of Szeged*

²*Faculty of Physics, West University of Timisoara*

³*Department of General and Environmental Physics, University of Szeged*

Article Info

Received: 18.03.2013

Accepted: 30.03.2013

Keywords: Liquid Phase Pulsed Laser Ablation (LP-PLA), vanadium, nanostructure, fractal analysis methods (FAM), box count methods, fractal dimension

Abstract

Pulsed laser irradiated vanadium surface morphology under different ambient has been prepared and characterized using fractal dimension analysis method on scanning electron microscopy (SEM) images. In presence of different ambient, self-periodic and self-similar surface patterns (e.g. dots, islands, and pins) were grown and appeared in different shapes. The fractal dimension (FD) of this developed vanadium nanostructure was calculated by fractal box count method (FBM). The calculated fractal dimension (FD, D_f) shows dependence on the different type on ambient and the number of laser shots.

1. Introduction

In the last four decades vanadium and vanadium oxide become intensively studied materials due to their unique chemical and physical structures [1-4]. Their electronic and surface

characteristic made them valuable base material for wide range of application such as catalysis [5], electrochemistry [6], and potential possibilities in the rechargeable ion batteries [7] and electronics [8]. There are many growth techniques described in literature that are used to produce nanostructure from these materials [9, 10].

In the last four decade, shape characterization can be a useful method for identifying relevant information on imaging. One method, which is receiving increasing usage in last few years, is to characterize the shape complexity of the solids using a measure known as fractal dimension (FD). Fractal dimension analysis (FDA) was first made popular by a series of works by Benoit Mandelbrot in the late 1970s and early 1980s [11, 12]. These analytic techniques can capture very complicated structures using relatively simple computational algorithms. Scientists have used fractal analysis for many years to quantify geologic phenomena such as decay of coastlines, analyzing cracks in crystal structure, botanical simulation, and medical modeling [13]. The most known fractal-like properties are the self-similarity, self-periodicity, scale independencies with “fine” structures, can be better given recursively than classical geometrical methods. Fractal box count method (FBM) defines the box dimension (D_f , FD) value that is smaller than topological dimension value.

Purpose of this analysis is to apply a fractal analysis technique to high-resolution surface pattern images in order to quantify the alteration in shape of the ablated vanadium-oxide that creates variant morphology on surface. Images were provided by SEM and sixteen samples were taken under control and analyzed. These images were analyzed using semi-automated analysis software application. The fractal dimension (FD, D_f) of the nanostructures were then computed using a box-counting algorithm. The fractal measure has regional variability which reflects local differences in vanadium-oxide surface structure. Fractal dimension is complementary to surface or volumetric measures and may assist in identifying developing morphology state or possible progression the alteration.

2. Experimental

The nanostructures on vanadium surface had been generated by femto-second laser pulses using liquid phase pulsed laser ablation (LP-PLA) experimental method. The type of primer laser source was the EMG 150 Excimer laser. This laser was pumped a dye laser system [14]. The

parameter of the output beam: $\lambda=500$ nm, $\tau=480$ fs, $E=15$ mJ. The beam was directed through an alumina mirror and a convex focal lens (focal length was 135mm) perpendicularly to the vanadium target. The target was placed into the PTFE (Polytetrafluoroethylene) chamber top of the computer controlled x-y stage (Fig. 1.).

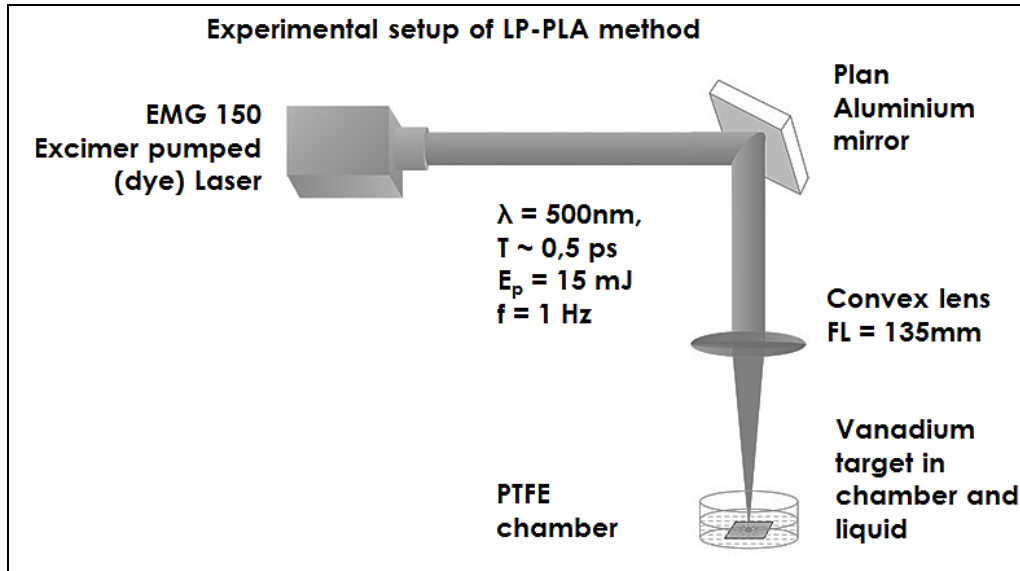


FIGURE 1. The schematic arrangement of the LP-LPA experimental setup.

Our vanadium (V) metallic thin film foils targets were Good Fellow Company (UK) with thickness of 0,2-0,4mm and purity 99% were used. The V foil surfaces before illumination were ultrasonically cleaned and bath in ethanol for 15 minutes to result clear surface for experiments. Four different ambient were used at room temperature, such as ethanol (ethyl alcohol), isooctane (trimethylpentane), deionized water and air (dry sample means sample without any liquids). In all cases of liquid ambient 20 ml of them were placed on the vanadium targets (it was 1cm height liquid layer on the metal surface). Change parameters were four different ambient material, position of the target and the number of laser shot. The laser pulse number was same (36, 72, 144, 288 pulse/time interval) for all samples with different ambient. The irradiated samples as fresh ones were immediately sent to microscopic investigation.

The nanostructure on the V foil surface had been generated by different number of laser pulses (1-1000). The surface morphology was investigated by scanning electron microscope (SEM) (Hitachi S4700). The topology of surface was studied by profilometry (Dektak 3 ST

Surface Profiler). The resulting surface morphology was studied by fractal analysis method (FAM). Provided images by the electron microscope are sized HxW=1280x960 pixels and were 16 bit RGB colored.

Fractal box dimension (FBD) method

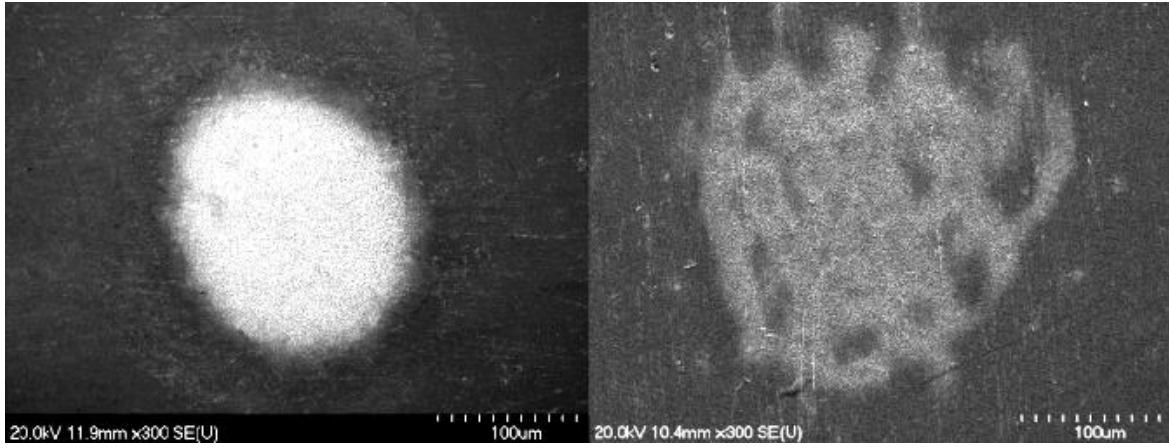
Fractal box dimension (FD, D_f) is defined with the following equation:

$$D_f^{BOX} = -\lim_{\varepsilon \rightarrow 0} \left(\frac{\ln(N_\varepsilon(S))}{\ln \varepsilon} \right) = -\lim_{\varepsilon \rightarrow 0} \left(\frac{\ln(\text{box counts})}{\ln(\text{size of box})} \right) \quad (1)$$

S is an n-dimensional set. In case of n=1 then S is a line (1D). If n=2 then S is a surface (2D) and when n=3 then S is a volume (3D) in the physical space. The ε is an n-dimensional cube side-length, where $\varepsilon > 0$ and $\varepsilon \rightarrow 0$. N is a minimum number of n-dimensional cubes with side-length ε to cover S set. The ‘box counts’ argument means the calculated number of boxes in an investigated image by a fixed box size and the ‘size of box’ argument means one of linear dimensions (edge of the box) of each box (where BS value can be one of {64,128, 256, 512} pixel values) are used in our calculation process actually.

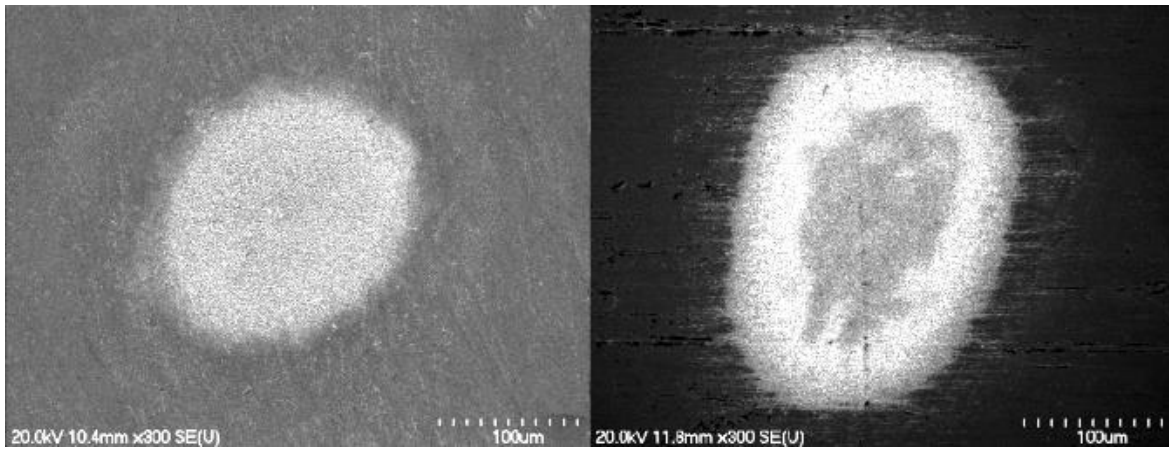
Image processing

In this study we examined the fractal dimension in case of different laser shot number and different ambient material. The (Fig 2.) shows the electron microscopy pictures of the laser irradiated vanadium surfaces in case of dry (a) ethanol (b) isooctane (c) and water (d) respectively. The numbers of laser shots are increased in order (36, 72, 144 and 288).



(a)

(b)



(c)

(d)

FIGURE 2. SEM pictures of the laser irradiated V surface in case of different ambient: dry (a), ethanol (b), isooctane (c) water (d). The laser shot number is 288 for (a)-(d) cases.

The two-dimensional SEM images were converted to gray scale (on 8 bit the intensity depth (I) is 0-255 bit) where threshold level (TH):of images at first:

$$TH = 0,5(I_{max} - I_{min}) \quad (2)$$

In equation (2) I_{max} means the maximum value of pixel intensity and I_{min} means the minimum value of pixel intensity in the histogram.

Next that the gray images converted to binary black & white image (b&w) where the black pixels represents the background (BG) part while the white pixels mean the foreground (FG) part. Threshold levels (TH) between white and black pixels were set automatically for each images based on the given formula above. Prior to analysis of the resulted figures we have done this whole procedure on all the SEM images. The analysis has carried out by our Matlab software and ImageJ application. Our working program fills a series of grids with decreasing box size ($BS = \{64, 128, 256, 512\}$) over an image. After that, the program counts the number of boxes on the image using one of actual BS values that falls on the image furthermore it calculates the number of pixels per box for each box size and for each grid. Finally, the program scans an image multiple times over different grid position. In our analysis we do not use smoothing filter. Six grids were selected and automatically analyzed by the software.

Our computational steps can be summarizing from (i) to (v) explaining in the following four steps. First, (i) the information subtitles of the images were cut down for getting clear pixel area, thus image size H is reduced to 986 pixel size. In step (ii) all RGB color images were converted to 8-bit grayscale. In the next step (iii) for getting some desired segmentation of image, a TH was set up by our application for each image. This TH calculated from the dark background level (BG) and white foreground (FG) level pixel numbers, using $TH = 0.5(BG + FG)$ equation ((2) above). After getting TH level (iv) images were converted to binary (b&w). In final step (v) we using default TH level and do analyze (BCA) method with twelve different box size settings such as $\{2, 3, 4, 6, 8, 12, 16, 32, 64, 128, 256, 512\}$ and then we got computed FD data in order. The result plots as shown in (Fig. 3. to Fig. 6.).

To complete image processing part of our discussion we need to take into consideration the errors of image processing of FBM. In this place we do not want to go into all details only to emphasize related errors the box count method. In this topic a suggested summary overview is [16]. For our fractal surface of V film, only a finite resolution is available, so the limit of $\varepsilon \rightarrow 0$ cannot be taken. Approximation is just to apply (1) directly but with the smallest ε available. So, that is $D_f^{BOX} \approx \ln[1/N(\varepsilon)] / \ln[\varepsilon]$. The problem with this approximation is that it converges with logarithmic slowness in ε . The negative slope of this curve will give D_f^{BOX} for small ε , thus $D_f^{BOX} \approx - \Delta[\ln(N(\varepsilon))] / \Delta[\ln(\varepsilon)]$. Other element of the accuracy of the sample size itself, because of

finite $N (= HxW)$ pixel number is available. Let $n(\varepsilon)$ be the number of nonempty boxes and $n'(\varepsilon)$ the number of boxes inside which at least one of the sample pixel lies. The natural approximation in this case is to estimate $n(\varepsilon)$ with $n'(\varepsilon, N)$. Here, although $n'(\varepsilon, N)$ clearly underestimates $n(\varepsilon)$, it is expected to be a good approximation for large N since for fixed ε . The $n(\varepsilon) = \lim (n'(\varepsilon, N))$ where $N \rightarrow \infty$. The finite sample is a serious limitation because, particularly for multifractals that are nonuniformly populated with pixel points, the limit in last given equation converges slowly. Grassberger has fitted the form $n(\varepsilon) - n'(\varepsilon, N) \sim \varepsilon^\alpha N^\beta$ with α and β parameters [17]. The dependence of accuracy with respect to the size of the available data set (N) is function of the number of available pixel points (N) and the real error $\sim 1/N^\alpha$ where parameter α denotes the exponent of the inverse power fit. Furthermore we calculate correlation coefficients (R) for the polynomial fits in the plots.

3. Results and discussion

According to SEM images, the shape and density of formed structure had been easily influenced by varying the ambient material, pulse number and energy flux [15]. Since the modified surfaces show some self-similar characteristic features could be considered as a fractal object. Hence, FAM seemed to be obvious to apply.

The SEM images are proved the self-similarities in the structure of the nanostructures on vanadium surfaces. The FAM calculation-processes have been done for all samples and all selected SEM images with magnification value 1000 ($M=1000$). The results are shown on (Fig. 3.) in case of dry ambient. At the left side of the figure (A) the pure results of FD calculation can be seen as the function of laser pulse number. The fractal dimension shows a decreasing value as the laser pulse number increase. However the maximum dimension value produced at 72 number of laser shots. This figure shows the effect of the box size in the FAM calculation. The shown size number on the figures concerns the pixel number of the box edge used in calculation. It is shown that the box size (BS) does not any significant effect on the value of fractal dimension (FD). We can see the average value of these fractal dimensions at (Figure 3. B.). The fitted polynomial curve is also shown on this figure. We can see the decreasing type of the calculated function.

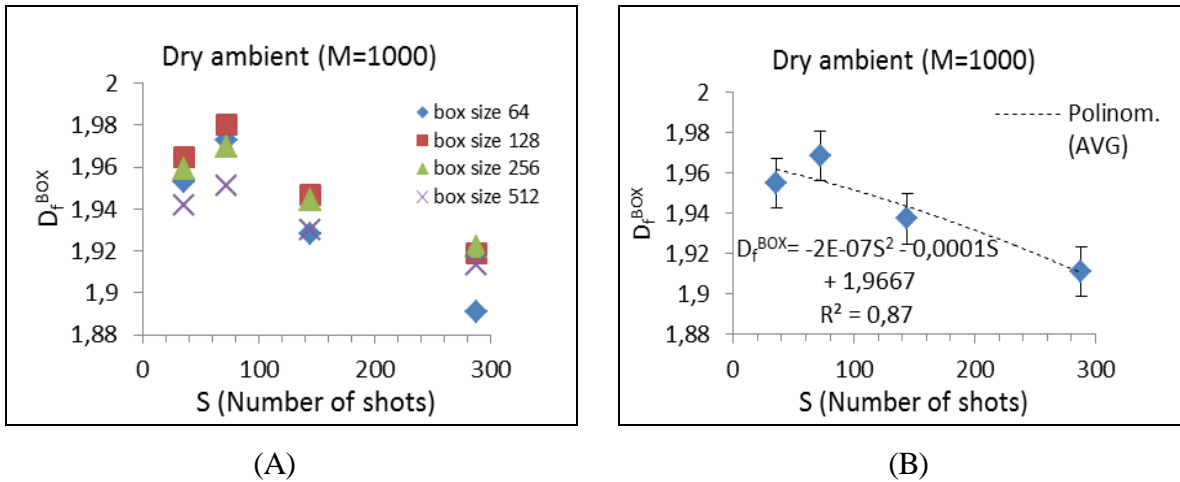


FIGURE 3. Results of FAM calculation in case of dry ambient.

The (Fig 4.) shows same type of results on fractal dimension calculation in case of water ambient. The shape of the fractal dimension vs. laser pulse number functions shows slightly same characteristic as in case of air ambient. The decreased part starts also over 72 laser shots. However the value of the calculated fractal dimension is little bit different from the air ambient case. This similarity indicate that the nanostructure formation processes results same surface characteristic. This means that the nanostructure formation under water ambient on vanadium surface is slightly same as in air ambient.

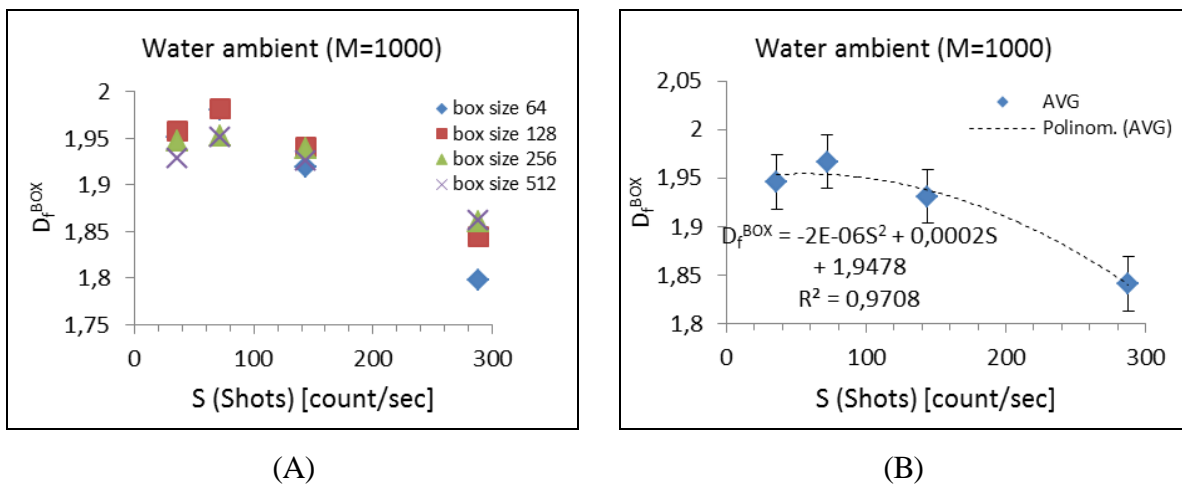


FIGURE 4. Results of FAM calculation in case of water ambient.

Our next ambient material was the isooctane. The results of the fractal dimension calculation concerning to this material case is shown on (Fig. 5.). In this case we get different results as in the previous cases. The Fractal dimension value is decrease with the laser pulse numbers until 144 laser pulses. From this number of laser shots the dimension value starts to increase.

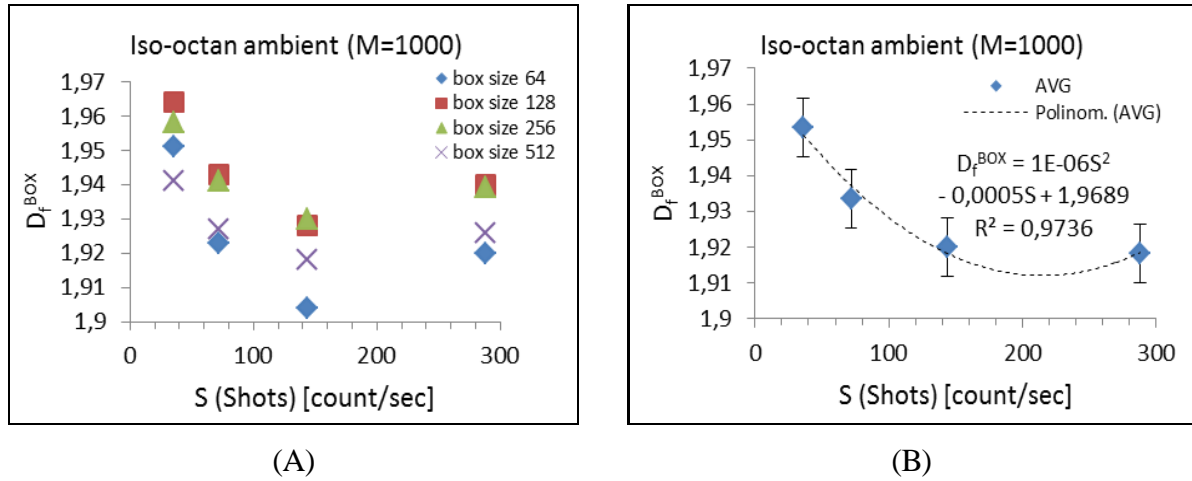
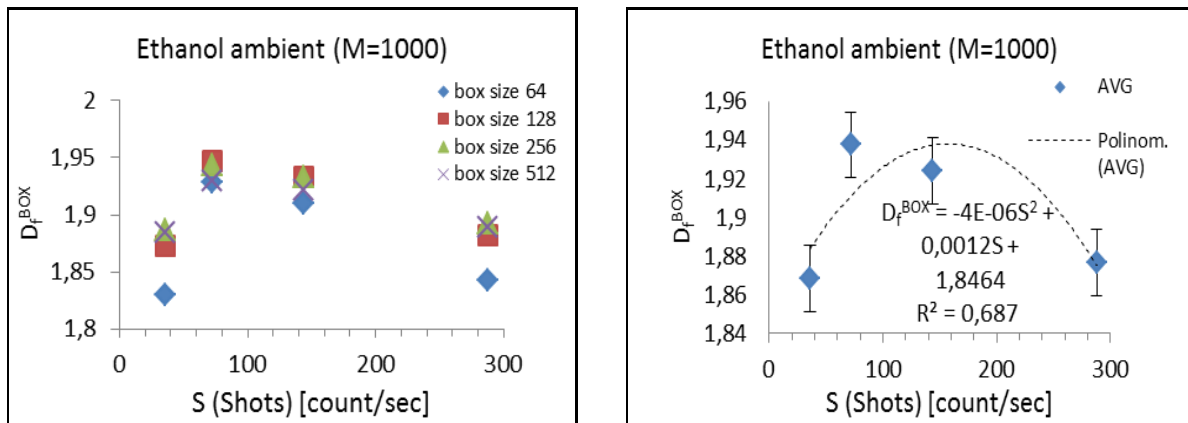


FIGURE 5. Results of FAM calculation in case of isooctane ambient.

The final case of this study we used ethanol as ambient material on vanadium target. The fractal dimension of the laser formed nanostructures shows a third type functions (Fig. 6) on the laser pulse number. In this case the fractal dimension shows also decreasing relations with the laser shot numbers but the shape of this curve is different from the air or water ambient.



(A)

(B)

FIGURE 6. Results of FAM calculation in case of ethanol ambient.

Applied different ambient in the LP-PLA (Liquid Phase Pulsed Laser Ablation) method result slightly different surface morphology on pure vanadium surface in case of carbon consist ambient. The air and water ambient have mostly same resulted fractal dimension dependence on laser pulse number.

The evaluation of pattern structures of metal surfaces due to interference of polarized laser-matter interaction have been observed in - almost - all samples independently of ambient. The size and heights of pattern were shown a little dependence (increasing) on the number of laser shots. More detailed structures were observed in case of liquid ambients probably because of limited heat convections and irradiations at liquid-solid interface.

4. Conclusion

The surface morphology of vanadium sample using different ambient was studied by fractal dimension analysis. The fractal dimension changed according to the nanostructure of the ablated surface. The fractal box dimension D_f^{BOX} and the surface pattern continuity (integrity) may decrease above a certain threshold number of shots in case of ambient (i.e. case of water and air) used changed in growth process. FAM has proved oneself as an acceptable technique to show the changes in this time period. The D_f^{BOX} using different ambient FBM not only reflects the morphology of nanostructures, but also shows changes according to the material of ambient. Thin V film sample under liquid layer with prefocused laser pulses causes a smooth and even surface. However, D_f^{BOX} with using ethanol and iso-octan under this threshold value of shot numbers contribute for developing of surface and the D_f^{BOX} is increased. This characteristic seems to be reliable in process of preparing metal oxide structures for different (e.g. catalytic) applications.

Acknowledgement

This work was supported by University of Szeged, Gyula Juhász Teacher Training Faculty under contact number: 2S753 1601, 2S511 1601. The work was also supported by Hungarian Government in frame of TÁMOP-4.2.2.A-11/1/KONV-2012-0060 program. The authors are indebted to Prof. I. Hevesi and S. Szatmari for their careful discussions.

References

- [1] Hu, J.; Odom, T. W.; Lieber, C. M., *Acc. Chem. Res.* 1999, 32, 435-445.
- [2] Odom, T. W.; Huang, J.-L.; Kim, P.; Lieber, C. M. *J. Phys. Chem. B* 2000, **104**, 2794-2809
- [3] Beth S. Guiton, Qian Gu, Amy L. Prieto, Mark S. Gudiksen, and Hongkun Park Single-Crystalline Vanadium Dioxide Nanowires with Rectangular Cross Sections, *J. Am. Chem. Soc.* 9 Vol. **127**, No. 2, 2005
- [4] S. Beke, L. Kőrösi, S. Papp, A. Oszkó, L. Nánai: XRD and XPS analysis of laser treated vanadium oxide thin films. *Applied Surface Science*, **255**, 9779-9782 (2009)
- [5] Chakrabarti, K. Hermann, R. Druzinic, M. Witko, F. Wagner, and M. Petersen: Geometric and electronic structure of vanadium pentoxide: A density functional bulk and surface study, *Phys. Rev. B* **59**, 10583–10590 (1999)
- [6] Yifu Zhang, Meijuan Fan, Min Zhou, Chi Huang, Chongxue Chen, Yuliang Cao, Guangyong Xie, Houbin Li And Xinghai Liu: Controlled synthesis and electrochemical properties of vanadium oxides with different nanostructures, *Bull. Mater. Sci.*, Vol. **35**, No. 3, June 2012, pp. 369–376.
- [7] Sanja Tepavcevic, Hui Xiong, Vojislav R. Stamenkovic, Xiaobing Zuo, Mahalingam Balasubramanian, Vitali B. Prakapenka, Christopher S. Johnson, and Tijana Rajh: Nanostructured Bilayered Vanadium Oxide Electrodes for Rechargeable Sodium-Ion Batteries, *ACS Nano*, 2012, **6** (1), pp 530–538
- [8] Junqiao Wu. "Metal-Insulator Phase Transition in Vanadium Dioxide for Electronics". Talk or presentation, 19, April, 2012. Spring E3S Research Seminar Series.
- [9] Janicskó-Csáthy J., Sajti Cs., George T.F., Nánai L.: Laser-driven growth of oxide micro- and nanostructures. *Annual Meeting of American Material Physics Society*, Indianapolis (IN), 14-18 March 2002, D-8

- [10] Wang, Z.L. Nanobelts, nanowires and nanodiskettes of semiconducting oxides - from materials to nanodevices. *Adv. Mater.* 2003, **15**, 432-436.
- [11] Mandelbrot B. B.; *Fractals: Form, chance, and dimension*. San Francisco: W. H. Freeman; 1977.
- [12] Mandelbrot B. B. *The fractal geometry of nature*. San Francisco: W.H. Freeman; 1982.
- [13] Herbert DE, Croft P. *Chaos and the changing nature of science and medicine: An introduction*: Mobile, AL, April 1995. Woodbury, N.Y: AIP; 1996.
- [14] S. Szatmári: High-brightness ultraviolet excimer lasers., *Appl. Phys B* **58**, 211-223, pp. 211-223
- [15] B. Farkas, M. Füle, Agneta M. Balint, L. Nánai: Laser fabricated surface nanostructure on vanadium foil. Universitatea de Vest din Timisoara Facultatea de Fizica. *Physics Conference TIM-10*, Timisoara (RO), 25-27 Nov 2010
- [16] J. Theiler: Estimating fractal dimension, *J. Opt. Soc. Am. A*, Vol. **7**, No. 6 , pp 1065 (1990)
- [17] P. Grassberger: On the fractal dimension of the Henon attractor, *Phys. Lett. A* **97**, 224 (1983)